Hepatic PLIN5 signals via SIRT1 to promote autophagy and prevent inflammation during fasting[S]

Enxiang Zhang,*,† Wenqi Cui,† Michael Lopresti,† Mara T. Mashek,† Charles P. Najt,† Hongbo Hu,[1,*] and Douglas G. Mashek[1,†,§]

Beijing Advanced Innovation Center for Food Nutrition and Human Health,* College of Food Science and Nutritional Engineering, China Agricultural University, Beijing, People's Republic of China; and Departments of Biochemistry, Molecular Biology, and Biophysics† and Medicine,§ Division of Diabetes, Endocrinology, and Metabolism, University of Minnesota, Minneapolis, MN

ORCID ID: 0000-0002-2780-5568 (H.H.)

Abstract **Lipid droplets (LDs) are energy-storage organelles that are coated with hundreds of proteins, including members of the perilipin (PLIN) family. PLIN5 is highly expressed in oxidative tissues, including the liver, and is thought to play a key role in uncoupling LD accumulation from lipotoxicity; however, the mechanisms behind this action are incompletely defined. We investigated the role of hepatic PLIN5 in inflammation and lipotoxicity in a murine model under both fasting and refeeding conditions and in hepatocyte cultures. PLIN5 ablation with antisense oligonucleotides triggered a pro-inflammatory response in livers from mice only under fasting conditions. Similarly, PLIN5 mitigated lipopolysaccharide- or palmitic acid-induced inflammatory responses in hepatocytes. During fasting, PLIN5 was also required for the induction of autophagy, which contributed to its anti-inflammatory effects. The ability of PLIN5 to promote autophagy and prevent inflammation were dependent upon signaling through sirtuin 1 (SIRT1), which is known to be activated in response to nuclear PLIN5 under fasting conditions. Taken together, these data show that PLIN5 signals via SIRT1 to promote autophagy and prevent FA-induced inflammation as a means to maintain hepatocyte homeostasis during periods of fasting and FA mobilization.**—Zhang, E., W. Cui, M. Lopresti, M. T. Mashek, C. P. Najt, H. Hu, and D. G. Mashek. **Hepatic PLIN5 signals via SIRT1 to promote autophagy and prevent inflammation during fasting.** ***J. Lipid Res.*** **2020.** 61: **338–350.**

Supplementary key words fatty acids • lipid droplets • lipotoxicity • perilipin 5 • sirtuin 1

Intracellular lipid droplets (LDs) are energy-storage organelles composed of a core of neutral lipids surrounded by a phospholipid monolayer embedded with hundreds of proteins. LD accumulation in non-adipose tissue is tightly linked to numerous metabolic diseases, including type 2 diabetes (1), and is the defining characteristic of nonalcoholic fatty liver disease (NAFLD) (2). While LDs themselves are often considered inert, a growing body of literature shows that dysregulation of lipid metabolic pathways leading to the accumulation of intermediates in triacylglycerol (TAG) metabolism can trigger lipotoxicity and impair cellular homeostasis. In addition, the presence of specific proteins on the surface of LDs can couple/uncouple LD accumulation and cellular dysfunction. Perilipins (PLINs) are a family of constitutive LD proteins comprised of five members. PLIN2 is the most abundant isoform in the liver, and its expression is tightly correlated with LD abundance and NAFLD (3). Ablation of PLIN2 reduces hepatic LD accumulation and prevents NAFLD and related complications, suggesting a role for PLIN2 in linking LDs to cellular dysfunction (4, 5). In contrast, the presence of PLIN5 on LDs can uncouple LD accumulation from metabolic dysregulation. PLIN5 overexpression in liver, muscle, or heart promotes LD accumulation but prevents insulin resistance (6, 7); whereas, liver-specific ablation of PLIN5 causes insulin resistance despite reduced LD accumulation (8). Both PLIN2 and PLIN5 affect LD metabolism, at least in part,

This study was supported by National Institutes of Health Grants DK114401 and AG055452 and American Diabetes Association Grant 1-16-IBS-203 to D.G.M, National Natural Science Foundation of China Grant 31671945 to H.H, and China Scholarship Council Grant 201706350184 to E.Z. The content is solely the responsibility of the authors and does not necessarily represent the official views of the National Institutes of Health. The authors declare that they have no conflicts of interest with the contents of this article.

Manuscript received 15 August 2019 and in revised form 9 January 2020.

Published, JLR Papers in Press, January 13, 2020
DOI https://doi.org/10.1194/jlr.RA119000336

Abbreviations: ASO, antisense oligonucleotide; CQ, chloroquine; IL, interleukin; IPA, Ingenuity Pathways Analysis; LD, lipid droplet; LPS, lipopolysaccharide; NAFLD, nonalcoholic fatty liver disease; PA, palmitic acid; PLIN, perilipin; SIRT1, sirtuin 1; TAG, triacylglycerol.

The data discussed in this publication have been deposited in NCBI's Gene Expression Omnibus (Zhang et al., 2019) and are accessible through GEO Series accession number GSE140024 (http://www.ncbi.nlm.nih.gov/geo/query/acc.cgi?acc=GSE140024).

[1]To whom correspondence should be addressed.
e-mail: dmashek@umn.edu (D.G.M.); hongbo@cau.edu.cn (H.H)

[S] The online version of this article (available at https://www.jlr.org) contains a supplement.

through their inhibition of cytosolic lipases (9), which may explain why ablation of either PLIN2 or PLIN5 lowers hepatic LD accumulation. However, PLIN5 also serves a critical role in signaling through sirtuin 1 (SIRT1), a protein deacylase that influences a myriad of cellular functions. Specifically, following PKA-mediated phosphorylation, PLIN5 translocates to the nucleus where it interacts with and promotes the activity of SIRT1 and the transcriptional complex of PGC1-α/PPAR-α to increase the expression of downstream target genes governing mitochondrial biogenesis and oxidative metabolism (10). This increase in mitochondrial number and function may be a key factor in uncoupling LD accumulation from insulin resistance and cellular dysfunction.

Hepatic inflammation is associated with the majority of acute and chronic liver diseases. Lipid accumulation in response to high fat feeding leads to subacute hepatic inflammation via NF-κB activation with increased downstream cytokines such as TNF-α, interleukin (IL)-6, and IL-1β (11). It is recognized that high levels of FAs, especially saturated FAs such as palmitate, induce lipotoxicity and metabolic dysfunction and are major contributors to hepatic inflammation (12). The increased inflammatory signaling is both a hallmark and driver of more advanced liver diseases, including nonalcoholic steatohepatitis.

Autophagy is a catabolic pathway involving the degradation of cellular components during nutrient deprivation. Since the initial discovery that autophagy can modulate LD catabolism, in a process termed lipophagy (13), a rapidly growing body of literature has further defined this pathway and highlighted the importance of autophagy in the development of numerous diseases, including NAFLD. It is well-known that autophagy is suppressed in NAFLD, and numerous studies utilizing genetic approaches or dietary phytochemicals to promote autophagy have shown beneficial effects on the prevention or treatment of NAFLD in animal models (14, 15). Because alterations in LD dynamics, autophagy, and inflammation are key components of NAFLD, we sought to further investigate the mechanism through which PLIN5 regulates these factors under normal feeding conditions. Herein, we report that PLIN5 promotes fasting-induced autophagy and prevents FA-induced inflammation as a means to uncouple LD accumulation from metabolic dysfunction.

MATERIALS AND METHODS

Animals and diet

Eight-week-old male C57BL/6N mice were purchased from Charles River Laboratories and housed under controlled temperature and lighting (20–22°C; 10:14 h light-dark cycle) and with free access to water. All mice were maintained at the University of Minnesota Animal Facilities in accordance with the Institutional Animal Care Guidelines and all experimental procedures were approved by the Institutional Animal Care and Use Committee at the University of Minnesota. All mice were fed with the control purified diet (TD.94045; Harlan Teklad, Madison, WI). Control and PLIN5 antisense oligonucleotides (ASOs; Ionis Pharmaceuticals) were given via intraperitoneal injection twice per week at a dose of 40 mg/kg. After 3 weeks, all mice were euthanized for liver tissue and serum collection after overnight fasting or overnight fasting followed by 4 h refeeding. Where noted, leupeptin (40 mg/kg) was administered through intraperitoneal injection 4 h prior to euthanization to inhibit autophagy.

Cell culture and treatment

All cells were maintained in a humidified incubator at 37°C, 5% CO_2. AML-12 cells were obtained from the ATCC (Manassas, VA). Cells were grown in DMEM:F12 (1:1) supplemented with 10% FBS and ITS (10 μg/ml insulin, 5.5 μg/ml transferrin, 5 ng/ml selenium). Mouse primary hepatocytes were isolated by collagenase perfusion method from 10- to 12-week-old male C57BL/6 mice with free access to water and chow diet. Hepatocytes were plated on collagen-coated multi-well tissue culture plates for 4 h with M199 plating medium (Invitrogen) that contained 23 mM HEPES, 26 mM sodium bicarbonate, 10% FBS, 1% penicillin/streptomycin, 100 nM dexamethasone, 100 nM insulin, and 11 mM glucose. M199 maintenance medium contained 23 mM HEPES, 26 mM sodium bicarbonate, 1% penicillin/streptomycin, 5.5 mM glucose, 100 μM carnitine, 10 nM dexamethasone, and 10 nM insulin. To overexpress PLIN5, primary hepatocytes were transduced with either AAV blank control virus or PLIN5 produced by Applied Biological Materials Inc. with the backbone plasmid pAAV-G-CMV-SV40-GFP for 24 h in maintenance medium. Lentivirus expressing mCherry or mCherry-PLIN5 was produced by the Viral Vector and Cloning Core facility at the University of Minnesota. The plasmid pLV-EF1a-IRES-Puro (a gift from Dr. Tobias Meyer; Addgene plasmid #85132) was used as the backbone for the cloning of the mCherry-PLIN5 construct. Orientation and sequence were confirmed for the full ORF with Sanger sequencing. Then AML-12 cells were infected for 72 h followed by puromycin selection to generate the PLIN5 overexpressed cell line.

RNA isolation, RT-PCR, and real-time quantitative PCR analysis

RNA was extracted with TRIzol from liver tissues followed by reverse transcription with Super Script III First-Strand Synthesis Super-Mix (Invitrogen). Gene expression was measured and quantified using a SYBR Green ER Two-Step quantitative RT-PCR kit (Invitrogen) and an Applied Biosystems Step One Plus real-time PCR system. Data were analyzed using the delta-delta CT method. For all analyses, gene expression was normalized to ribosomal protein L32. Melting curve analysis was performed on all samples to verify primer specificity.

Protein isolation and Western blotting

Samples were lysed with ice-cold RIPA buffer and protein concentrations were determined by BCA assay. After electrophoretic separation, proteins were transferred to a nitrocellulose membrane and subsequently incubated with primary antibodies (PLIN5, LAMP1, p62, LC3, ATG7) and appropriate secondary antibodies. The immune-reactive bands were detected using enhanced chemiluminescence (Fisher/Pierce, Rockford, IL) and recorded with a Licor image system. Membranes were stained with Ponceau S, which was quantified by densitometry and used for normalization. For all studies, representative Western blots are shown and quantification is from n = 3–4.

Hepatic TAG measurement

Liver samples were homogenized in sterile water and extracted twice with chloroform:methanol (2:1). The chloroform layer was transferred, dried under nitrogen gas, and resolved in diluted Triton X-100. Colorimetric assays were used to quantify liver TAG (Stanbio).

LD staining

AML-12 cells were treated with 400 μM palmitic acid (PA) complexed to BSA (133 μM) or BSA alone overnight and then fixed with PBS containing 4% paraformaldehyde, followed by staining with LipidTOX™ Green and DAPI for subsequent confocal imaging.

IHC and histological analysis

Liver tissue was fixed with PBS containing 4% paraformaldehyde and embedded in paraffin. The paraffin-embedded tissue was processed for H&E and CD45 staining. Fresh liver tissue was needed for Oil Red O staining. ImageJ (National Institutes of Health) was used for image quantifications.

Autophagy flux measurement

AML-12 cells were transfected with pMRX-IP-GFP-LC3-RFP-LC3ΔG [a gift from Noboru Mizushima (16)] for 24 h with Lipofectamine 2000 (Invitrogen) according to the manufacturer's instructions. After transfection, cells were fixed with 4% paraformaldehyde followed by confocal imaging.

NF-κB activity assay

AML-12 cells were seeded at 1×10^5 cells per well in 24-well plates the day before transfection. All transfections were carried out with Lipofectamine 2000 (Invitrogen) according to the manufacturer's instructions. Cells were transfected with 80 ng of pMirReport luciferase expression construct containing the 3′ UTR of murine NF-κB and 20 ng pRL-SV40 Renilla luciferase vector (Promega E2231). Twenty-four hours after transfection, luciferase activities were measured using the Dual-Luciferase Reporter Assay System (Promega) and normalized to Renilla luciferase activity. All experiments were performed in triplicate.

RNA extraction, library preparation, and next-generation sequencing

RNA was extracted from snap-frozen liver tissue using the RNEasy RNA mini kit purchased from Qiagen. A total of 20 RNA samples (5 replicates from 4 treatment groups) were sent to the University of Minnesota Genomics Core for quality check, library preparation, and sequencing. Eukaryotic RNA isolates were quantified using a fluorometric RiboGreen assay. The total RNA integrity was assessed using capillary electrophoresis. Only samples higher than 1 μg with a RIN of 8 or greater proceeded to sequencing. Total RNA samples were converted to Illumina sequencing libraries using Illumina's Truseq RNA sample preparation kit. One microgram of total RNA was oligo-dT purified using oligo-dT-coated magnetic beads, fragmented, and then reverse transcribed into cDNA. The cDNA was fragmented, blunt-ended, and ligated to indexed (barcoded) adaptors and amplified using 15 cycles of PCR. Final library size distribution was validated using capillary electrophoresies and quantified using fluorimetry (Pico Green) and via quantitative (q)PCR. Indexed libraries were then normalized, pooled, and size selected to 320 bp using a Caliper XT instrument. Truseq libraries were hybridized to a single read flow cell, and individual fragments were clonally amplified by bridge amplification on the Illumina cBot. Once complete, the flow cell was loaded on the Hi-Seq 2500 and sequenced. Upon completion of read 1, an 8 bp forward and 8 bp reverse (i7 and i5) index read was performed. Base call files for each cycle of sequencing were generated by Illumina Real Time Analysis (RTA) software. Primary analysis and demultiplexing were performed using Illumina bcl2fatstq software version 2.17.1.14.

For the RNA sequencing analysis, 50 bp Fast Q Reads (n = 12 million per sample) were trimmed using Trimmomatic (v 0.33) enabled with the optional "-q" option; 3 bp sliding-window trimming from the 3′ end requiring minimum Q30. Quality control checks on raw sequence data for each sample were performed with Fast QC. Read mapping was performed via Bowtie (v2.2.4.0) using the UCSC mouse genome (mm10) as reference. Gene quantification was done via Cuffquant for FPKM values and Feature Counts for raw read counts. Differentially expressed genes were identified using the edge R (negative binomial) feature in CLCGWB (Qiagen) using raw read counts. The generated list was filtered on the basis of a minimum 2xAbs fold change and Bonferroni corrected $P < 0.05$. These filtered genes were then imported to Ingenuity Pathways Analysis (IPA) software (Qiagen) for pathway identification. Isoforms that exhibited a log2-fold change greater than 1 and an FDR less than 0.05 were subjected to IPA. The RNa-Seq dataset is deposited in GEO (GSE140024).

Statistical analysis

Statistical analysis was performed using GraphPad Prism 8. Data are expressed as mean ± SEM. Statistical analyses were performed using Student's *t*-test or two-way ANOVA where appropriate. $P < 0.05$ was considered statistically significant.

RESULTS

Hepatic deficiency of PLIN5 reduces LD abundance

To determine the roles of hepatic PLIN5 in fasting/refeeding metabolism, we employed ASOs to ablate PLIN5 expression in liver. Treatment with PLIN5 ASOs for 3 weeks reduced the expression of PLIN5 to undetectable levels and fasting increased PLIN5 expression (**Fig. 1A**). PLIN5 ablation had no effect on body weight or liver weight during the 3 week treatment period (Fig. 1B, C); PLIN5 ASOs mildly reduced adipose PLIN5 expression, but no changes in weight of the various adipose depots were observed (supplemental Fig. S1). Overnight fasting increased hepatic LD accumulation and TAG content compared with refeeding as expected, and PLIN5 ASO-treated mice had reduced abundance of hepatic LDs and TAG content in both fasted and refed conditions (Fig. 1D–F). Consistent with reduced LD accumulation, PLIN5 ablation reduced and overexpression increased FA incorporation into LD TAG (supplemental Fig. S2), suggesting that these alterations in FA esterification may contribute to the lower hepatic TAG observed in mice lacking PLIN5 in the liver.

Hepatic PLIN5 silencing produces distinct transcript profiles in response to fasting or refeeding

To identify global effects of PLIN5 knockdown under the different feeding conditions, we conducted RNA-Seq analysis of liver samples. IPA of the RNA-Seq data was employed to identify the key pathways changed in response to PLIN5 knockdown. We observed a total of 36 genes changed in the refeed condition in the mice administered PLIN5 ASOs with the majority of these being downregulated (**Fig. 2A**, C). In contrast, PLIN5 ablation under fasting conditions altered the expression of 136 transcripts with 78 being upregulated and 56 downregulated (Fig. 2A). Of the genes changed as a result of PLIN5 knockdown, only 10 were altered under both feeding conditions (Fig. 2B). Principal component analysis revealed that the gene-expression profiles were significantly separated between control and

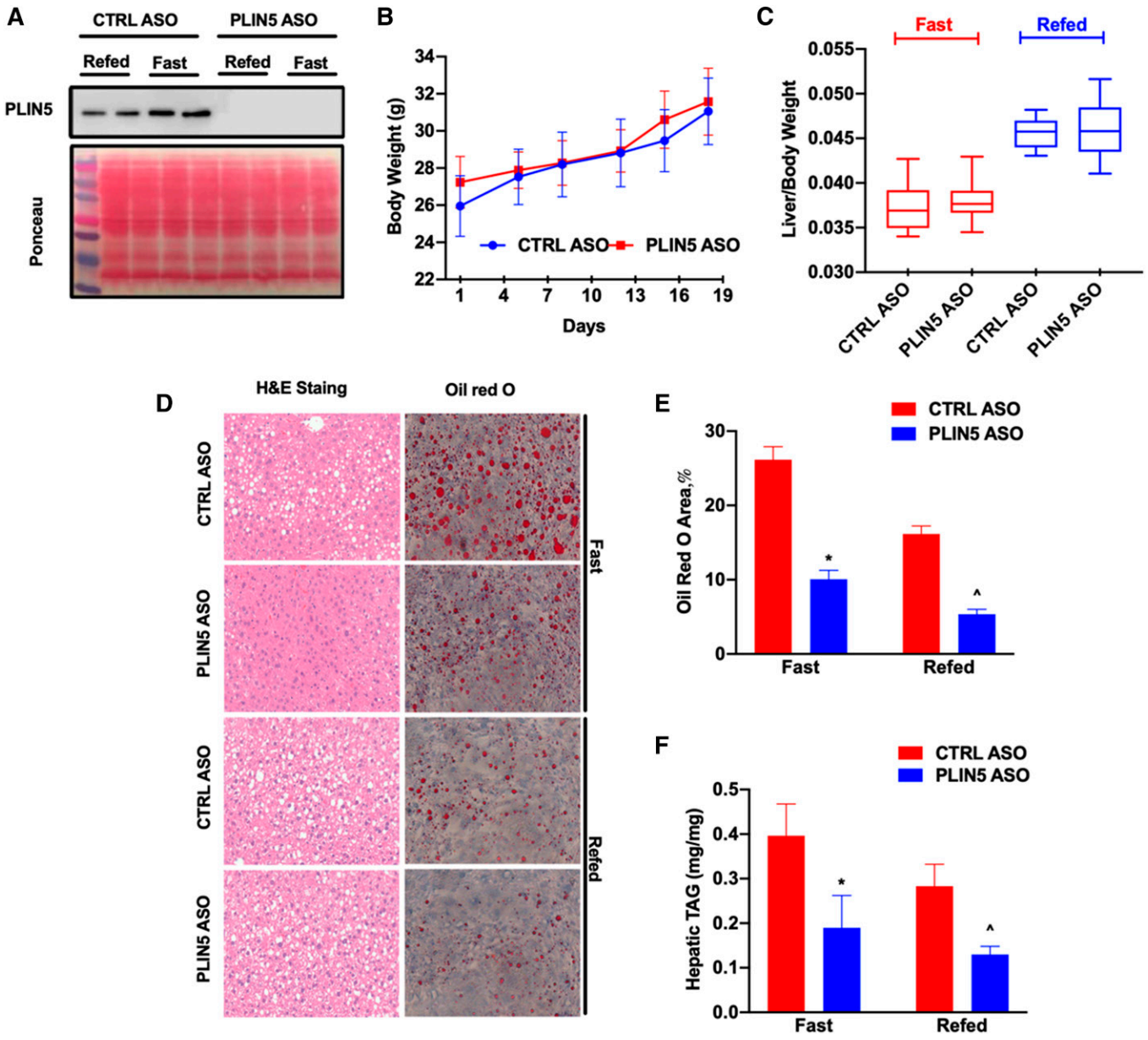

Fig. 1. Hepatic deficiency of PLIN5 decreases LD accumulation. A: Western blotting of PLIN5 in liver samples from fasted (Fast) or refed mice treated with control (CTRL) or PLIN5 ASO. B, C: Body weight and liver weight were not influenced by either fasting or refeeding conditions or PLIN5 ablation. D, E: PLIN5 deficiency reduced LD abundance as shown in H&E and Oil Red O staining. F: Enzymatic determination of hepatic TAG. *$P < 0.05$ versus CTRL ASO, ^$P < 0.05$ versus Fast (n = 6).

PLIN5 ASO-treated mice specifically under fasting conditions (Fig. 2D, E). As such, further analysis was focused on the effects of PLIN5 during fasting.

PLIN5 ablation promotes inflammation during fasting

Additional analysis of the RNA-Seq dataset revealed that there was a robust increase of pro-inflammatory transcripts in PLIN5 knockdown livers compared with control ASO (**Fig. 3A**). Consistent with this, inflammation-related pathways (acute phase response, hepatic fibrosis/stellate cell activation, GADD45 signaling, atherosclerosis signaling) were upregulated in response to PLIN5 knockdown during fasting (Fig. 3B). To further validate the involvement of PLIN5 in inflammation regulation, we examined several classic inflammatory signal markers in the liver including IL-1β, TNF-α, and IL-6, which were not significantly altered in the RNA-Seq dataset in the entire cohort of mice. All three transcripts of the inflammation-related markers were upregulated in livers following PLIN5 knockdown (Fig. 3C). Additionally, the leukocyte marker CD45 was increased with PLIN5 knockdown, suggesting increased hepatic immune cell infiltration (Fig. 3D, E). Treatment of isolated primary hepatocytes with lipopolysaccharide (LPS) reduced PLIN5 mRNA levels, which is consistent with PLIN5 having an anti-inflammatory role (Fig. 3E). In agreement with the studies in mice, PLIN5 knockdown in primary hepatocytes increased the pro-inflammatory response to LPS, as indicated by increased expression of IL-1β, TNF-α,

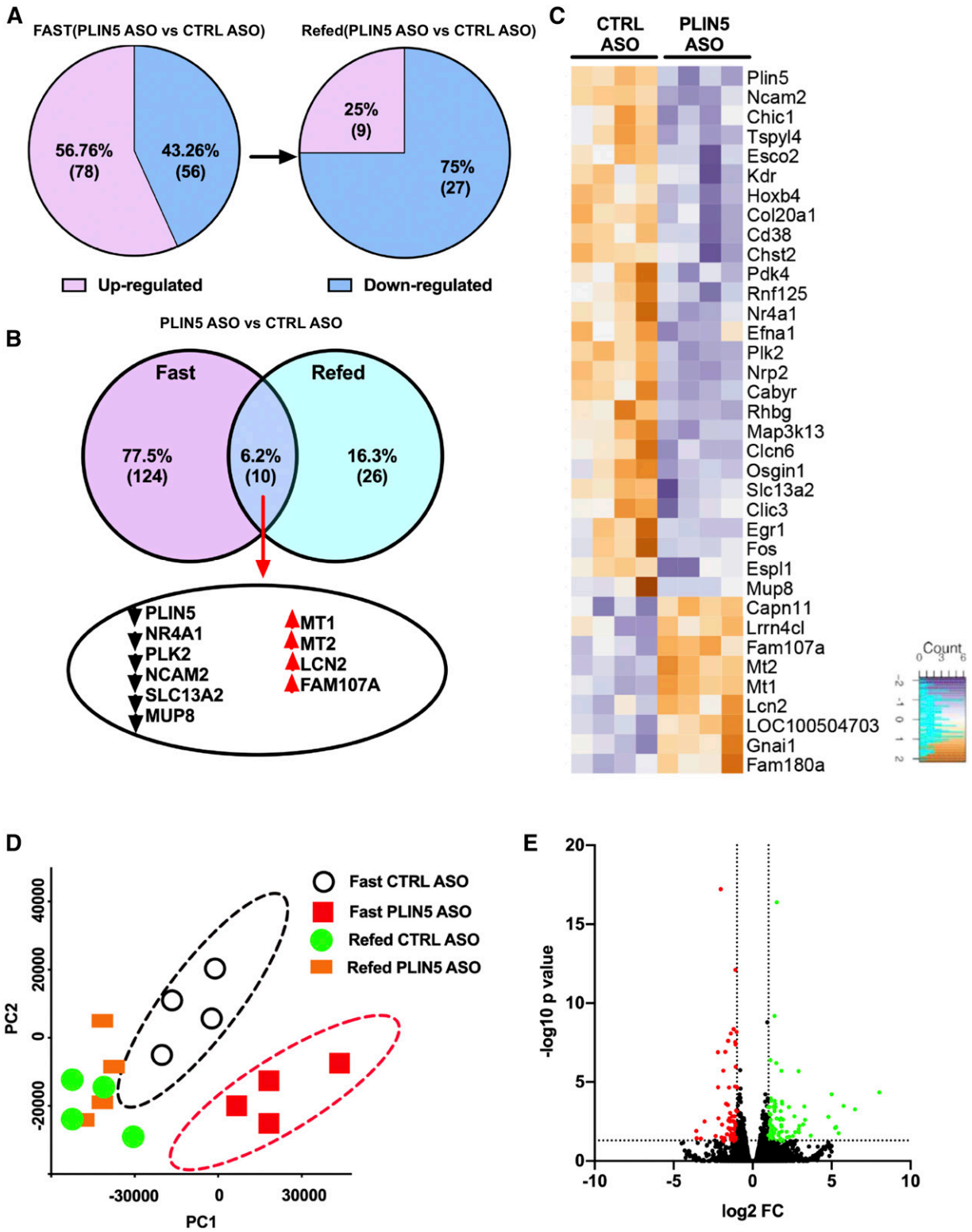

Fig. 2. Genome-wide gene expression analyses indicate a more important role of PLIN5 during fasting. A: RNA-Seq results showing differentially expressed genes in fasted (Fast) or refed conditions in response to hepatic PLIN5 knockdown. B: Venn diagram showing common genes altered following PLIN5 knockdown in both fed and fasted conditions. C: Heat map of changes in expression of genes changed by PLIN5 knockdown in the refed mice. D: Principal component analysis of the transcriptome showed the significant difference between mice treated with control (CTRL) or PLIN5 ASO in fasting condition. E: Volcano plot of transcriptomes from fasting liver. The downregulated genes are shown in red (upper left) and upregulated genes are shown in green (upper right). The x axis represents the log2-fold change of the genes. The y axis represents the −log10 of the *P* values (n = 4).

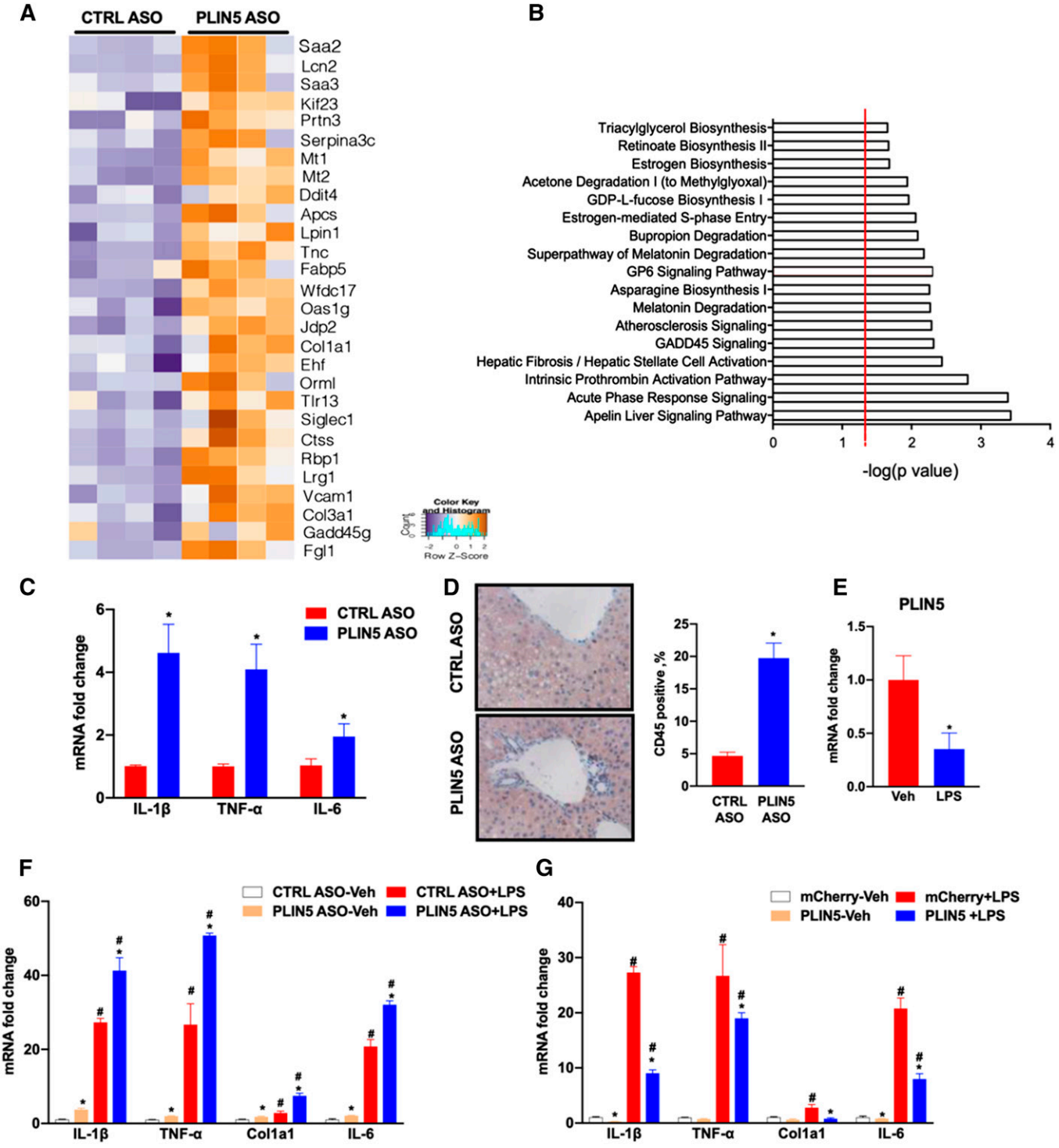

Fig. 3. PLIN5 ablation promotes inflammation. A: Heat map of inflammatory genes, derived from RNA-Seq analysis, in response to knockdown of PLIN5 in fasting mouse liver. The color scale shows fold change of gene expression in a purple-white-orange (from low to high expressions) scheme. B: RT-PCR analysis of classic inflammation markers including IL-1β, IL-6, and TNF-α in liver tissues of mice treated with ASOs. C, D: CD45 staining and quantification in liver samples. E: Abundance of PLIN5 mRNA in primary hepatocytes following 24 h of LPS exposure. For B, D, and E, $^{*}P < 0.05$ (n = 3–4). F: LPS-induced inflammatory responses in primary hepatocytes treated with ASOs (n = 3). G: LPS-induced inflammatory responses in AML-12 cells treated with lentiviruses (n = 3). For F and G, $^{*}P < 0.05$ versus control (CTRL) ASO or mCherry; $^{\#}P < 0.05$ versus vehicle (Veh).

Col1a1, and IL-6 in cells treated with PLIN5 ASOs (Fig. 3F). In contrast, PLIN5 overexpression attenuated LPS-induced inflammatory gene expression (Fig. 3G). Collectively, these data show that PLIN5 protects against LPS- or fasting-induced inflammation.

PLIN5 is required for fasting-induced autophagy

While autophagy was not a pathway that was significantly altered according to the IPA, we noted that many autophagy genes had lower expression in response to PLIN5 ablation, although they were below the 2-fold change threshold

(**Fig. 4A**). To further interrogate this pathway, we determined whether expression of protein markers of autophagy were changed accordingly. Ablation of PLIN5 reduced the expressions of ATG7, LAMP1, and LC3II/I while increasing p62, all of which are consistent with reduced autophagy (Fig. 4B, C). To decipher the effects of PLIN5 on autophagic flux, we administered leupeptin to mice 4 h prior to euthanization. Leupeptin induced the abundance of p62 and LC3II as expected, but PLIN5 knockdown attenuated this increase (Fig. 4D, E). In addition, PLIN5 ablation reduced autophagy flux in hepatocytes as measured by the RFP-GFP-LC3 reporter assay (Fig. 4F, G; supplemental Fig. S3A). We next overexpressed PLIN5 to determine whether its expression was enough to drive autophagy. PLIN5 overexpression increased LC3II/I and reduced p62, and treatment with leupeptin showed that these changes reflected increased autophagic flux (Fig. 4H–J, supplemental Fig. S3A). Taken together, these data show for the first time that PLIN5 plays a key role in regulating fasting-induced autophagy.

PLIN5 regulates inflammation partially through changes in autophagy

Given that liver-specific PLIN5 deficiency could promote acute inflammatory responses and inhibit autophagy induction, we examined whether these two signals were related. To do this, we treated primary hepatocytes with LPS and measured markers of autophagy and inflammation. We found that LPS treatment for both 6 and 24 h induced p62 accumulation and reduced the LC3II/I ratio, indicating inhibition of autophagy (**Fig. 5A–**C). However, 6 h treatment with LPS did not alter the mRNA expression of known inflammation markers (Fig. 5D), suggesting that PLIN5 deficiency suppressed autophagy prior to inflammation. To further test the relationship between autophagy and inflammation induction, we treated control and PLIN5-overexpressing AML-12 cells with LPS for 24 h (supplemental Fig. S2B). We found that overexpression of PLIN5 increased basal levels of protein markers of autophagy and attenuated the decrease in autophagy following LPS treatment, as shown by the LC3II/I ratio and LAMP1 level (Fig. 5E–G). Additionally, we measured NF-κB luciferase-reporter assay and expression of inflammatory genes in response LPS and/or chloroquine (CQ), an autophagy inhibitor, in primary hepatocytes (Fig. 5H, I). As expected, treatment with either LPS or CQ enhanced NF-κB activity, which was further elevated when LPS and CQ were combined. PLIN5 knockdown increased and PLIN5 overexpression reduced reporter activity in response to CQ or LPS individually, but the effects of PLIN5 were mildly attenuated with the combination of both drugs. Moreover, the ability of PLIN5 overexpression to reduce LPS-induced expression of pro-inflammatory genes was attenuated in the absence of CQ, suggesting that the induction of autophagy may contribute to the anti-inflammatory effects of PLIN5 (Fig. 5J–L).

PLIN5 attenuates the effects of PA-induced lipotoxicity

It is well-established that saturated FAs, especially PA, promote inflammation and are drivers of lipotoxicity (17). Given that PLIN5 knockdown promoted inflammation during fasting, when FA levels are high, we investigated whether altered PLIN5 expression was capable of modulating PA-induced inflammation. Acute exposure to PA or knockdown of PLIN5 increased expression of IL-1β, TNF-α, and IL-6 in primary hepatocytes as expected (**Fig. 6A**). However, PA elicited a more robust increase in inflammatory gene expression when PLIN5 was ablated. Consistent with these data, overexpression of PLIN5 significantly attenuated the increase in inflammatory gene expression in response to PA in AML-12 cells (Fig. 6B). These data suggest that the presence of PLIN5, which is normally increased upon fasting, is critical to mitigate FA-induced inflammation. The effects of PA on autophagy in the liver are less clear with studies showing that it either promotes or inhibits autophagy (18, 19). Exposure of primary hepatocytes to PA reduced autophagy; however, PLIN5 overexpression was able to partially offset these suppressive effects (Fig. 6C–E). Despite no effect of PLIN5 knockdown on TAG accumulation in response to PA (Fig. 6H–J), PLIN5 did mediate the effects of PA on ER stress in AML-12 cells. As measured by spliced XBP1 mRNA abundance and Bip protein expression, ER stress was robustly induced by PA as expected, but PLIN5 overexpression attenuated these effects (Fig. 6F–H). Thus, the presence of PLIN5 attenuates the detrimental effects of PA on autophagy suppression, inflammation, and ER stress.

PLIN5 regulates autophagy and inflammation via SIRT1

SIRT1 is well recognized as a major regulator of autophagy through its deacetylation of several proteins directly involved in autophagy as well a host of transcription factors that govern autophagy (20). PLIN5 interacts with SIRT1 under conditions such as fasting that promote cAMP/PKA signaling to increase SIRT1 activity (10). To investigate the relationship between PLIN5 and SIRT1, we infected primary hepatocytes with an adenovirus to overexpress PLIN5 and treated cells with EX527, a specific SIRT1 inhibitor. As expected, we observed an increase in the LC3II/I ratio and decreased p62 with PLIN5 overexpression, indicative of increased autophagy; however, treatment with EX527 abrogated these changes (**Fig. 7A–**C). Additionally, we utilized SIRT1 knockout MEFs to test the role of SIRT1 on PLIN5-mediated autophagy induction. PLIN5 overexpression in WT MEFs increased ATG7, LAMP1, and the LC3II/I ratio and decreased p62 accumulation, but these effects were not present in SIRT1 knockout cells (Fig. 7D–H). To test the involvement of SIRT1 in the PLIN5-driven inhibition of inflammation, we utilized the NF-κB Luc-reporter assay in WT MEFs and SIRT1 knockout cells. Consistent with earlier data, PLIN5 overexpression inhibited LPS- or PA-induced inflammation in WT MEFs, but not in SIRT1 knockout cells (Fig. 7I, J). Because SIRT1 deacetylates NF-κB/p65 to reduce its activity, we measured the acetylation status of NF-κB/p65. Relative to control ASO, PLIN5 ASO treatment increased NF-κB/p65 acetylation in fasted mice consistent with reduced signaling via SIRT1 (Fig. 7K). Collectively, these data show that PLIN5 signals via SIRT1 to promote autophagy and prevent inflammation (**Fig. 8**).

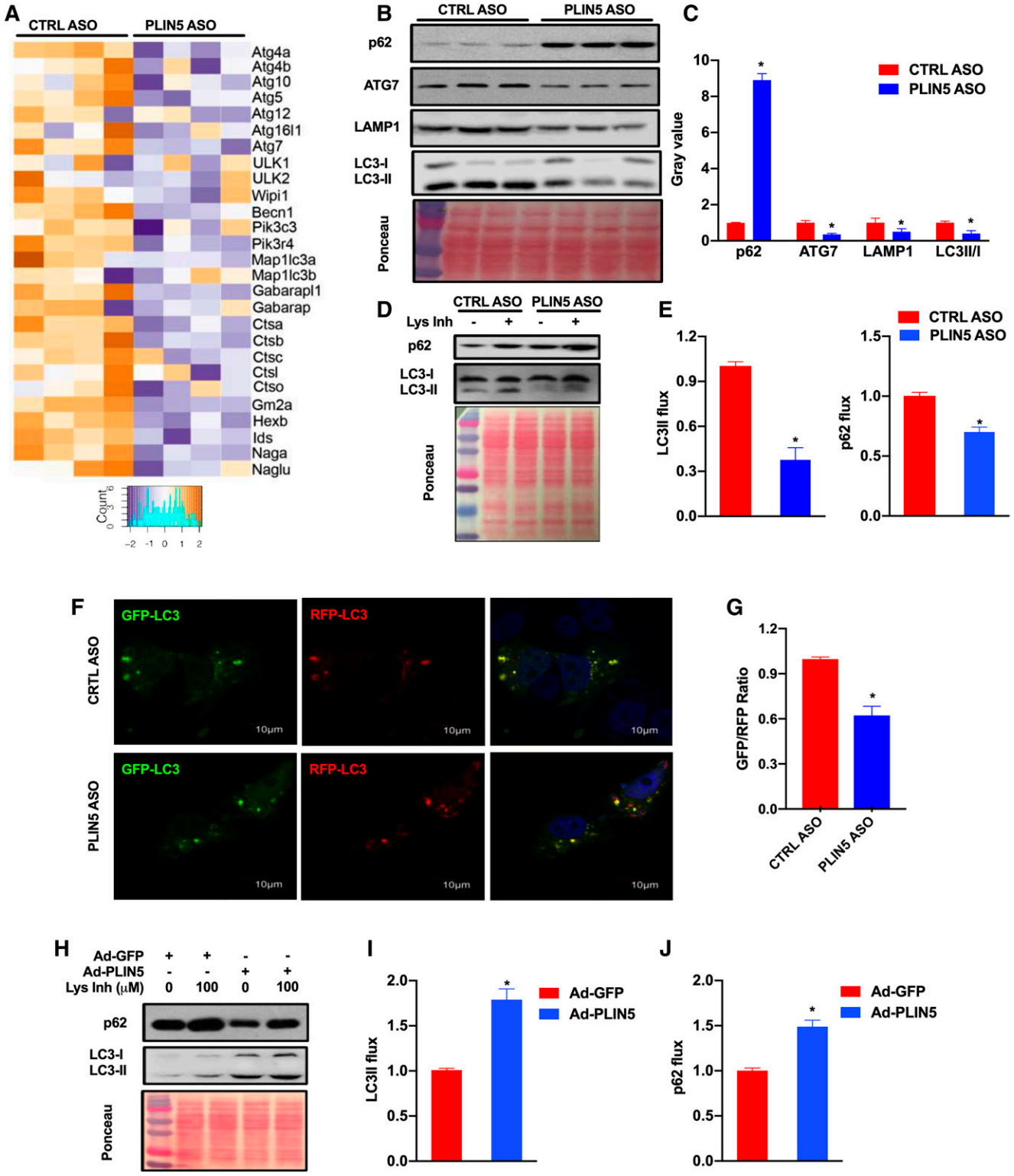

Fig. 4. PLIN5 deficiency in liver impairs autophagy under fasting conditions. A: Heat map of autophagy genes in response to PLIN5 ablation in fasting mouse livers. The color scale shows the fold change of gene expression in a purple-white-orange (from low to high expressions) scheme. B. C: Western blotting of autophagy-related proteins LC3II, ATG7, and LAMP1 and densitometry quantification; representative Western blot from three mice is shown. D, E: Western blotting and quantification of liver samples harvested from fasted mice that received leupeptin 4 h prior to euthanization to inhibit autophagy (n = 6). F, G: Hepatocytes were transfected with GFP-LC3-RFP-LC3ΔG plasmid to monitor the effects of PLIN5 in autophagic flux. H–J: Western blotting of autophagy proteins in tissue homogenates from primary hepatocytes overexpressing PLIN5; densitometry from n = 3. *$P < 0.05$ versus control (CTRL) ASO or Ad-GFP.

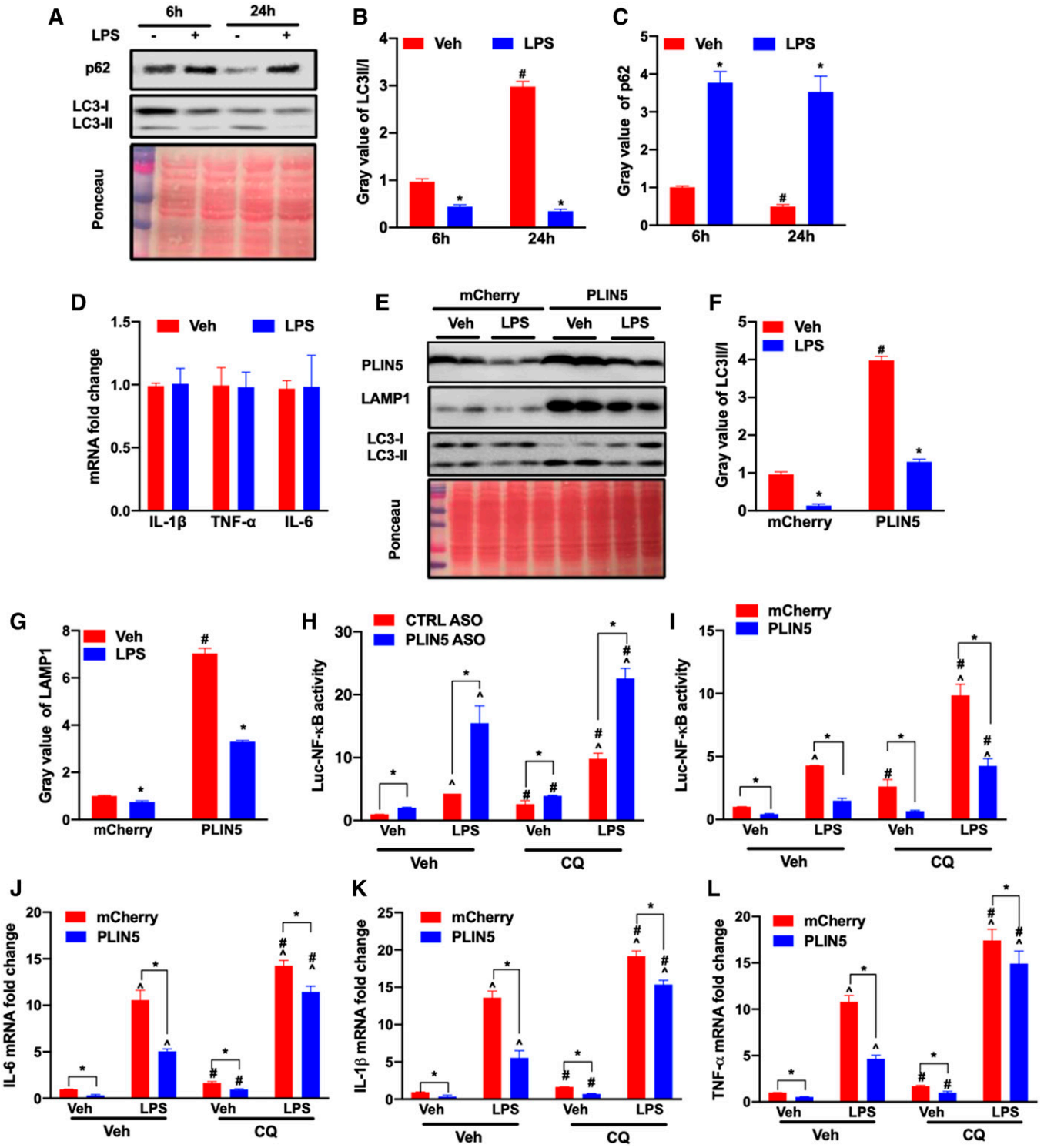

Fig. 5. PLIN5 regulates inflammation partially through changes in autophagy. A–C: Western blotting and densitometry for autophagy proteins in primary hepatocytes treated with LPS for 6 and 24 h. $^{*}P < 0.05$ versus vehicle (Veh); $^{\wedge}P < 0.05$ versus 6 h Veh. D: mRNA abundance of inflammatory genes in primary hepatocytes treated with LPS for 6 h. E–G: Western blotting and quantification of AML-12 cells treated with LPS and with PLIN5 overexpression (PLIN5). For B, C, F, and G, $^{*}P < 0.05$ versus Veh; $^{\#}P < 0.05$ versus 6 h or mCherry. H: NF-κB reporter activity in primary hepatocytes transfected with ASOs and treated with LPS and CQ. I: NF-κB reporter activity in primary hepatocytes transduced with lentiviruses and treated with LPS and CQ. For H and I, $^{*}P < 0.05$; $^{\wedge}P < 0.05$ versus Veh; $^{\#}P < 0.05$ versus Veh (CQ). J–L: Expression of endogenous NF-kB target genes. $^{*}P < 0.05$; $^{\wedge}P < 0.05$ versus within treatment Veh; $^{\#}P < 0.05$ versus double Veh (CQ) (n = 3–4 for A–L).

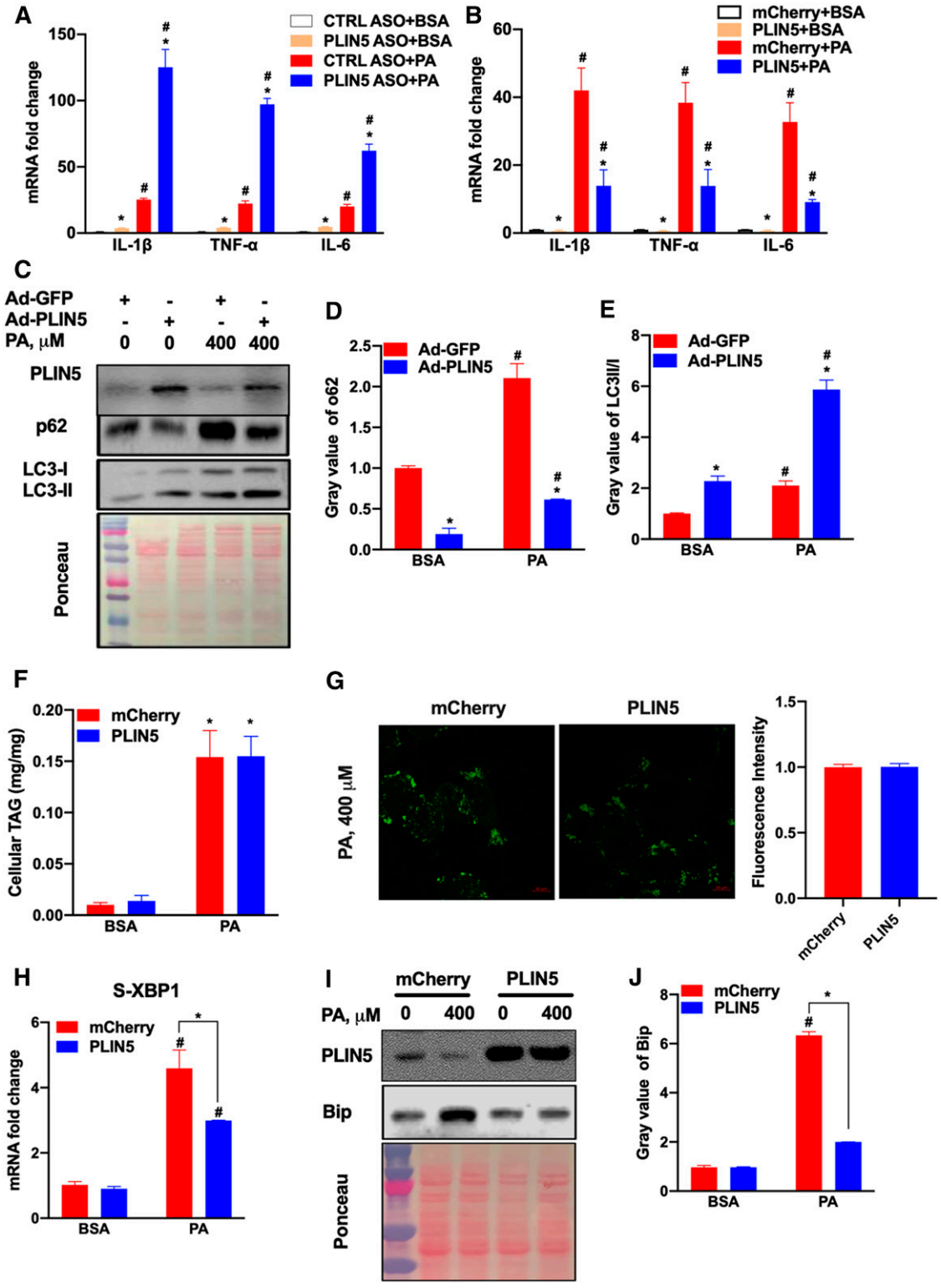

Fig. 6. PLIN5 attenuates LPS- and FA-induced inflammation and autophagy suppression. A: mRNA abundance of inflammatory genes in primary hepatocytes transfected with ASOs (0.5 μg/ml) that, after 48 h, were treated with PA for an additional 24 h. B: mRNA abundance of inflammatory genes in AML-12 cells transduced with lentiviruses and treated with PA. C–E: Western blotting and quantification of autophagy proteins in primary hepatocytes transduced with adenoviruses and treated with PA. *$P < 0.05$ versus control (CTRL) ASO, mCherry, or Ad-GFP; #$P < 0.05$ versus BSA. F: TAG concentration of AML-12 cells transduced with lentiviruses and treated with PA. *$P < 0.05$ versus BSA. G: LipidTOX™ staining of AML-12 cells transduced with lentiviruses and treated with PA. H: mRNA abundance of spliced XBP1 in AML-12 cells transduced with lentiviruses and treated with PA. *$P < 0.05$ versus mCherry; #$P < 0.05$ versus BSA. I, J: Western blotting of Bip and densitometry quantification (n = 3). *$P < 0.05$ versus mCherry; #$P < 0.05$ versus BSA (n = 3–4 for A–J).

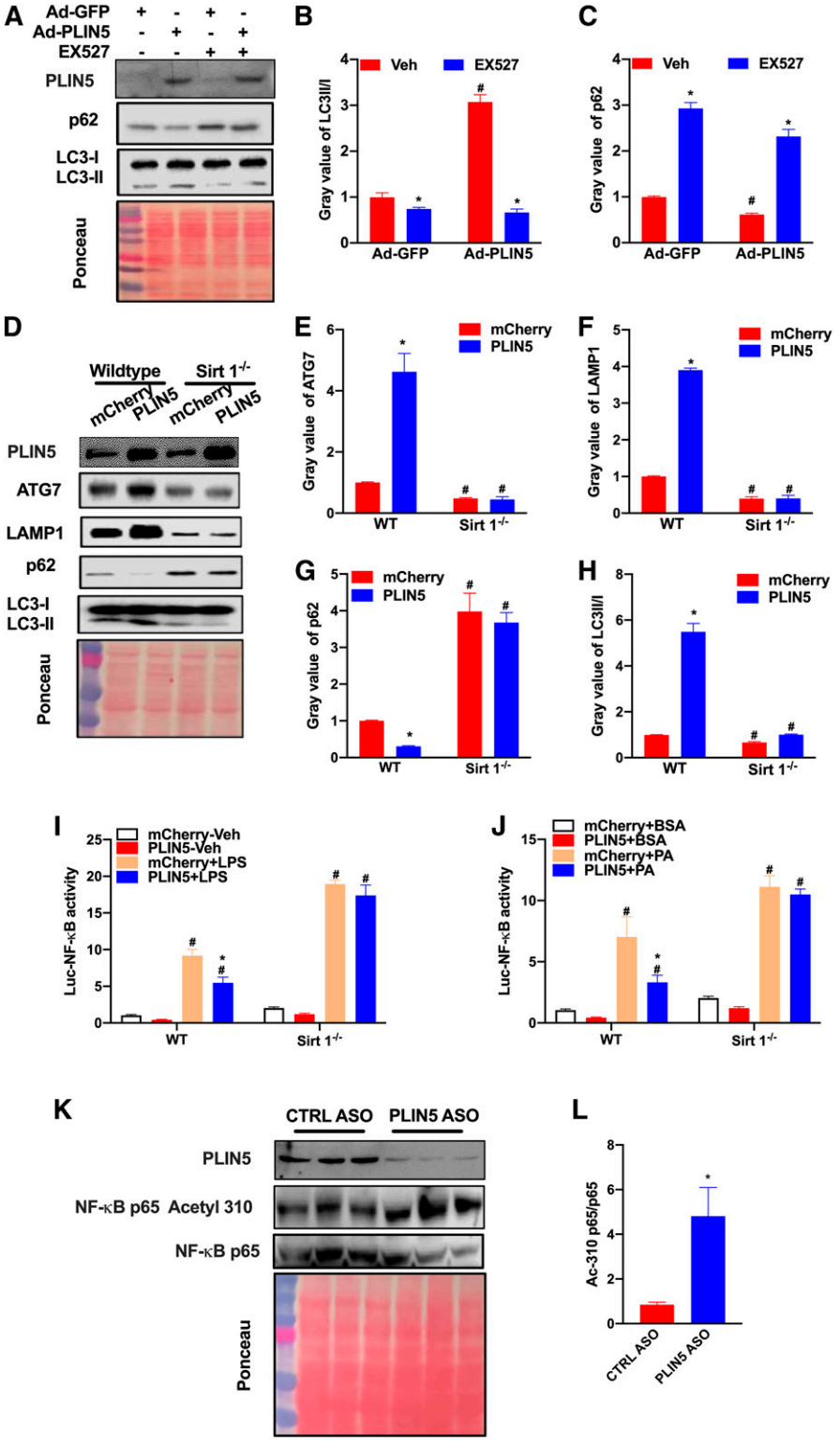

Fig. 7. SIRT1 mediates the effects of PLIN5 on autophagy induction and inflammation suppression. A–C: Western blotting and quantification of PLIN5 and autophagy proteins in primary hepatocytes transduced with adenoviruses and treated with the SIRT1 inhibitor EX-527. $^{*}P < 0.05$ versus vehicle (Veh); $^{\#}P < 0.05$ versus Ad-GFP. D–H: Western blotting and quantification of autophagy proteins in WT or SIRT1-null MEFs transduced with lentiviruses. $^{*}P < 0.05$ versus mCherry; $^{\#}P < 0.05$ versus WT. For A–H, n = 3–4. I: NF-κB reporter activity in MEFs transduced with lentiviruses and treated with LPS (n = 4). J: NF-κB reporter activity in MEFs transduced with lentiviruses and treated with PA (n = 4). For I and J, $^{*}P < 0.05$ versus mCherry; $^{\#}P < 0.05$ versus Veh. K, L: Western blotting of NF-κB or NF-κB (Acetyl 310) and densitometry quantification; representative Western blot from three mice is shown. $^{*}P < 0.05$ versus control (CTRL) ASO.

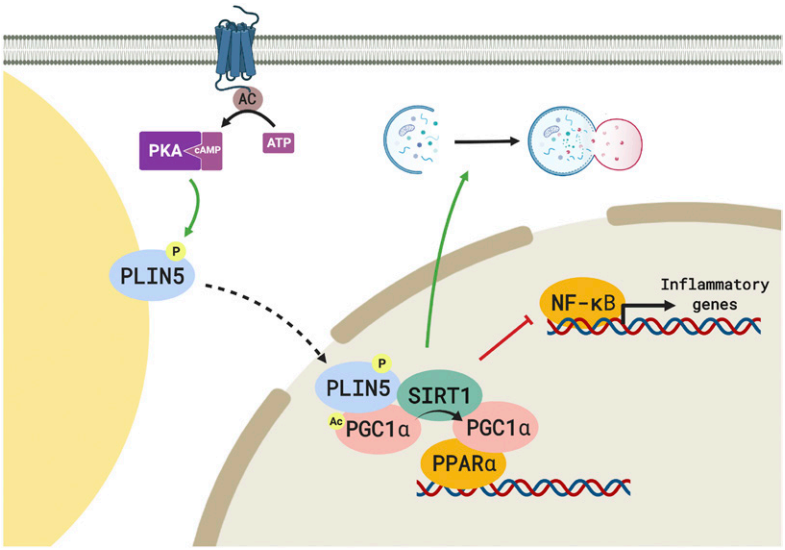

Fig. 8. Model. Upon fasting and subsequent PKA-mediated phosphorylation, PLIN5 translocates to the nucleus where it signals via SIRT1 to influence transcriptional networks (PGC-1α/PPAR-α among others) known to influence autophagy and inflammation. As a result, fasting-induced autophagy is promoted and inflammation is attenuated. Thus, PLIN5 appears to play an important role in mediating the response to extracellular inflammatory signals to maintain cell homeostasis.

DISCUSSION

These studies explored the function and regulatory roles of PLIN5 in the liver under different dietary conditions. The most robust effects of PLIN5 ablation were observed in response to fasting, with only subtle changes in gene expression observed upon refeeding. These data are consistent with the upregulation of PLIN5 expression during fasting (Fig. 1A) and increased PLIN5 phosphorylation in response to stimuli, such as fasting, that promote β-adrenergic signaling (21). We also observed that PLIN5 ablation reduced LD accumulation in both fed and fasted mice. These data are in line with previous studies showing that PLIN5 inhibits lipolysis (23) via PLIN5-mediated binding and inhibition of ATGL (24) and promotes FA incorporation into cellular TAG (8, 25).

PLIN5 ablation resulted in a comprehensive upregulation of inflammation in livers from fasted mice. PLIN5 ablation is documented to increase insulin resistance and mitochondrial dysfunction, which often coincide with inflammation (8, 26, 27). In addition, downstream signaling mediators of PLIN5, such as SIRT1, PGC-1α, and PPAR-α, have anti-inflammatory effects (28). Our data show that although PLIN5 regulates inflammation under basal conditions, the most robust effects are observed in response to inflammatory triggers such as LPS or PA. The ability of PLIN5 to attenuate inflammation in response to PA also suggests that the increase in fasting-induced inflammation in PLIN5-ablated livers may be due to an inability to respond to the elevated influx of FAs or the hormonal signaling required to facilitate metabolism of the incoming FAs. PLIN5 expression was also suppressed following LPS exposure suggesting that its downregulation may be a critical event to allow for robust inflammatory signaling.

A major finding of the current study is that PLIN5 knockdown robustly suppressed fasting-induced autophagy. While this is the first study to demonstrate a link between PLIN5 and autophagy, ample evidence exists that indirectly connects PLIN5 to the regulation of autophagy. PLIN5 phosphorylation and translocation in response to cAMP/PKA triggers its translocation to the nucleus to promote SIRT1 activity leading to increased PGC-1α/PPAR-α signaling and mitochondrial biogenesis (10). However, SIRT1 is also well-established to be a master regulator of autophagy (20) and is required for fasting-induced autophagy in the liver (29). When these studies are taken together, they provide a logical connection between PLIN5 and autophagy induction. Indeed, the current study not only demonstrates the critical role of PLIN5 on fasting-induced autophagy but also shows that these effects are dependent upon SIRT1, as either chemical or genetic inhibition of SIRT1 negates the effects of PLIN5. Consistent with a role for autophagy as a modulator of inflammation (30), we also found that autophagy is required for the full anti-inflammatory effects of PLIN5 in response to LPS or PA. Thus, the regulation of both autophagy and inflammation appear to play significant roles contributing to the overall effects of PLIN5.

In summary, these data highlight a critical role for PLIN5 in regulating fasting-induced autophagy and inflammation in the liver. Additionally, SIRT1 acts as a key node downstream of PLIN5 that links PLIN5 to alterations in both autophagy and inflammatory pathways. These data provide new insights into the mechanism underlying the beneficial effects of PLIN5 and provide further rationale for identifying therapies that activate the PLIN5-SIRT1 signaling axis as a means to prevent or treat diseases characterized by altered lipid metabolism and metabolic dysfunction.

The authors would like to thank the University of Minnesota Imaging Center and Juan Abrahante from the University of Minnesota for RNA-Seq analysis and the Viral Vector and Cloning Core facility at the University of Minnesota for help with developing the lentivirus.

REFERENCES

1. Greenberg, A. S., R. A. Coleman, F. B. Kraemer, J. L. McManaman, M. S. Obin, V. Puri, Q. W. Yan, H. Miyoshi, and D. G. Mashek. 2011. The role of lipid droplets in metabolic disease in rodents and humans. *J. Clin. Invest.* **121:** 2102–2110.

2. Mashek, D. G., S. A. Khan, A. Sathyanarayan, J. M. Ploeger, and M. P. Franklin. 2015. Hepatic lipid droplet biology: getting to the root of fatty liver. *Hepatology.* **62:** 964–967.
3. Fujii, H., Y. Ikura, J. Arimoto, K. Sugioka, J. C. Iezzoni, S. H. Park, T. Naruko, H. Itabe, N. Kawada, S. H. Caldwell, et al. 2009. Expression of perilipin and adipophilin in nonalcoholic fatty liver disease; relevance to oxidative injury and hepatocyte ballooning. *J. Atheroscler. Thromb.* **16:** 893–901.
4. Najt, C. P., S. Senthivinayagam, M. B. Aljazi, K. A. Fader, S. D. Olenic, J. R. Brock, T. A. Lydic, A. D. Jones, and B. P. Atshaves. 2016. Liver-specific loss of perilipin 2 alleviates diet-induced hepatic steatosis, inflammation, and fibrosis. *Am. J. Physiol. Gastrointest. Liver Physiol.* **310:** G726–G738.
5. Imai, Y., G. M. Varela, M. B. Jackson, M. J. Graham, R. M. Crooke, and R. S. Ahima. 2007. Reduction of hepatosteatosis and lipid levels by an adipose differentiation-related protein antisense oligonucleotide. *Gastroenterology.* **132:** 1947–1954.
6. Trevino, M. B., D. Mazur-Hart, Y. Machida, T. King, J. Nadler, E. V. Galkina, A. Poddar, S. Dutta, and Y. Imai. 2015. Liver perilipin 5 expression worsens hepatosteatosis but not insulin resistance in high fat-fed mice. *Mol. Endocrinol.* **29:** 1414–1425.
7. Pollak, N. M., M. Schweiger, D. Jaeger, D. Kolb, M. Kumari, R. Schreiber, S. Kolleritsch, P. Markolin, G. F. Grabner, C. Heier, et al. 2013. Cardiac-specific overexpression of perilipin 5 provokes severe cardiac steatosis via the formation of a lipolytic barrier. *J. Lipid Res.* **54:** 1092–1102.
8. Keenan, S. N., R. C. Meex, J. C. Y. Lo, A. Ryan, S. Nie, M. K. Montgomery, and M. J. Watt. 2019. Perilipin 5 deletion in hepatocytes remodels lipid metabolism and causes hepatic insulin resistance in mice. *Diabetes.* **68:** 543–555.
9. Sztalryd, C., and D. L. Brasaemle. 2017. The perilipin family of lipid droplet proteins: gatekeepers of intracellular lipolysis. *Biochim. Biophys. Acta Mol. Cell Biol. Lipids.* **1862 (10 Pt B):** 1221–1232.
10. Gallardo-Montejano, V. I., G. Saxena, C. M. Kusminski, C. Yang, J. L. McAfee, L. Hahner, K. Hoch, W. Dubinsky, V. A. Narkar, and P. E. Bickel. 2016. Nuclear perilipin 5 integrates lipid droplet lipolysis with PGC-1α/SIRT1-dependent transcriptional regulation of mitochondrial function. *Nat. Commun.* **7:** 12723.
11. Del Campo, J. A., P. Gallego, and L. Grande. 2018. Role of inflammatory response in liver diseases: therapeutic strategies. *World J. Hepatol.* **10:** 1–7.
12. Malhi, H., and G. J. Gores. 2008. Molecular mechanisms of lipotoxicity in nonalcoholic fatty liver disease. *Semin. Liver Dis.* **28:** 360–369.
13. Singh, R., S. Kaushik, Y. Wang, Y. Xiang, I. Novak, M. Komatsu, K. Tanaka, A. M. Cuervo, and M. J. Czaja. 2009. Autophagy regulates lipid metabolism. *Nature.* **458:** 1131–1135.
14. Khambu, B., S. Yan, N. Huda, G. Liu, and X. M. Yin. 2018. Autophagy in non-alcoholic fatty liver disease and alcoholic liver disease. *Liver Res.* **2:** 112–119.
15. Lin, C. W., H. Zhang, M. Li, X. Xiong, X. Chen, X. Chen, X. C. Dong, and X. M. Yin. 2013. Pharmacological promotion of autophagy alleviates steatosis and injury in alcoholic and non-alcoholic fatty liver conditions in mice. *J. Hepatol.* **58:** 993–999.
16. Kaizuka, T., H. Morishita, Y. Hama, S. Tsukamoto, T. Matsui, Y. Toyota, A. Kodama, T. Ishihara, T. Mizushima, and N. Mizushima. 2016. An autophagic flux probe that releases an internal control. *Mol. Cell.* **64:** 835–849.
17. Ertunc, M. E., and G. S. Hotamisligil. 2016. Lipid signaling and lipotoxicity in metaflammation: indications for metabolic disease pathogenesis and treatment. *J. Lipid Res.* **57:** 2099–2114.
18. Cai, N., X. Zhao, Y. Jing, K. Sun, S. Jiao, X. Chen, H. Yang, Y. Zhou, and L. Wei. 2014. Autophagy protects against palmitate-induced apoptosis in hepatocytes. *Cell Biosci.* **4:** 28.
19. Tanaka, S., H. Hikita, T. Tatsumi, R. Sakamori, Y. Nozaki, S. Sakane, Y. Shiode, T. Nakabori, Y. Saito, N. Hiramatsu, et al. 2016. Rubicon inhibits autophagy and accelerates hepatocyte apoptosis and lipid accumulation in nonalcoholic fatty liver disease in mice. *Hepatology.* **64:** 1994–2014.
20. Lee, I. H., L. Cao, R. Mostoslavsky, D. B. Lombard, J. Liu, N. E. Bruns, M. Tsokos, F. W. Alt, and T. Finkel. 2008. A role for the NAD-dependent deacetylase Sirt1 in the regulation of autophagy. *Proc. Natl. Acad. Sci. USA.* **105:** 3374–3379.
21. Bickel, P. E., J. T. Tansey, and M. A. Welte. 2009. PAT proteins, an ancient family of lipid droplet proteins that regulate cellular lipid stores. *Biochim. Biophys. Acta.* **1791:** 419–440.
22. Wang, H., and C. Sztalryd. 2011. Oxidative tissue: perilipin 5 links storage with the furnace. *Trends Endocrinol. Metab.* **22:** 197–203.
23. Wang, C., Y. Zhao, X. Gao, L. Li, Y. Yuan, F. Liu, L. Zhang, J. Wu, P. Hu, X. Zhang, et al. 2015. Perilipin 5 improves hepatic lipotoxicity by inhibiting lipolysis. *Hepatology.* **61:** 870–882.
24. Wang, H., M. Bell, U. Sreenivasan, H. Hu, J. Liu, K. Dalen, C. Londos, T. Yamaguchi, M. A. Rizzo, R. Coleman, et al. 2011. Unique regulation of adipose triglyceride lipase (ATGL) by perilipin 5, a lipid droplet-associated protein. *J. Biol. Chem.* **286:** 15707–15715. [Erratum. 2013. *J. Biol. Chem.* 288: 10952.]
25. Trevino, M. B., Y. Machida, D. R. Hallinger, E. Garcia, A. Christensen, S. Dutta, D. A. Peake, Y. Ikeda, and Y. Imai. 2015. Perilipin 5 regulates islet lipid metabolism and insulin secretion in a cAMP-dependent manner: implication of its role in the postprandial insulin secretion. *Diabetes.* **64:** 1299–1310.
26. Mason, R. R., R. Mokhtar, M. Matzaris, A. Selathurai, G. M. Kowalski, N. Mokbel, P. J. Meikle, C. R. Bruce, and M. J. Watt. 2014. PLIN5 deletion remodels intracellular lipid composition and causes insulin resistance in muscle. *Mol. Metab.* **3:** 652–663.
27. Trevino, M. B., D. Mazur-Hart, Y. Machida, T. King, J. Nadler, E. V. Galkina, A. Poddar, S. Dutta, and Y. Imai. 2015. Liver perilipin 5 expression worsens hepatosteatosis but not insulin resistance in high fat-fed mice. *Mol. Endocrinol.* **29:** 1414–1425.
28. Kauppinen, A., T. Suuronen, J. Ojala, K. Kaarniranta, and A. Salminen. 2013. Antagonistic crosstalk between NF-κB and SIRT1 in the regulation of inflammation and metabolic disorders. *Cell. Signal.* **25:** 1939–1948.
29. Sun, Y., M. Xia, H. Yan, Y. Han, F. Zhang, Z. Hu, A. Cui, F. Ma, Z. Liu, Q. Gong, et al. 2018. Berberine attenuates hepatic steatosis and enhances energy expenditure in mice by inducing autophagy and fibroblast growth factor 21. *Br. J. Pharmacol.* **175:** 374–387.
30. Peng, X., Y. Wang, H. Li, J. Fan, J. Shen, X. Yu, Y. Zhou, and H. Mao. 2019. ATG5-mediated autophagy suppresses NF-κB signaling to limit epithelial inflammatory response to kidney injury. *Cell Death Dis.* **10:** 253.